Macromolecules

pubs.acs.org/Macromolecules Article

C−H/C−H Oxidative Direct Arylation Polycondensation to Isoindigo-Based n-Type Conjugated Polymers

Yibo Shi, Xuwen Zhang, Tianzuo Wang, Mei Rao, Yang Han, Yunfeng Deng,* and Yanhou Geng*

Cite This: *Macromolecules* 2024, 57, 4158−4166 Read Online

ACCESS | Metrics & More | Article Recommendations | Supporting Information

ABSTRACT: Two high molecular weight conjugated polymers (CPs), i.e., poly[*N*,*N*′-bis(4-tetradecyloctadecyl)-7,7′-difluoroisoindigo-*alt*-2,2′-bithiazole] (P2FI2Tz) and poly[*N*,*N*′-bis(4-tetradecyloctadecyl)-5,5′,7,7′-tetrafluoroisoindigo-*alt*-2,2′-bithiazole] (P4FI2Tz), were synthesized via C−H/C−H oxidative direct arylation polycondensation (Oxi-DArP) using $PdCl_2$/CuCl/Cu$(OAc)_2$ as catalytic system and chlorobenzene as solvent. Both polymers are unipolar n-type semiconductors with electron mobility (μ_e) > 0.2 cm^2 V^{-1} s^{-1}, attributed to their low-lying highest occupied molecular orbitals (HOMOs) and lowest unoccupied molecular orbital (LUMOs), which are −6.01/−3.69 and −6.24/−3.82 eV for P2FI2Tz and P4FI2Tz, respectively. P2FI2Tz was also synthesized via C−Br/C−H direct arylation polycondensation (DArP) and Stille polycondensation. The resultant polymers P2FI2Tz-D and P2FI2Tz-S showed slightly lower μ_e compared to Oxi-DArP-made polymer (P2FI2Tz-O1) with a similar molecular weight. Notably, Oxi-DArP is much faster and more efficient than DArP and Stille polycondensation. P2FI2Tz with a number-average molecular weight (M_n) above 40 kDa, was obtained in 9 h of Oxi-DArP, significantly shorter than 24 h with DArP and Stille polycondensation. P2FI2Tz with a M_n as high as 191 kDa could be synthesized via Oxi-DArP by extending the polymerization time to 16 h. Our results prove Oxi-DArP to be an efficient protocol to synthesize polymer semiconductors. This is also the first comparative study on three methods, i.e., Oxi-DArP, DArP, and Stille polycondensation.

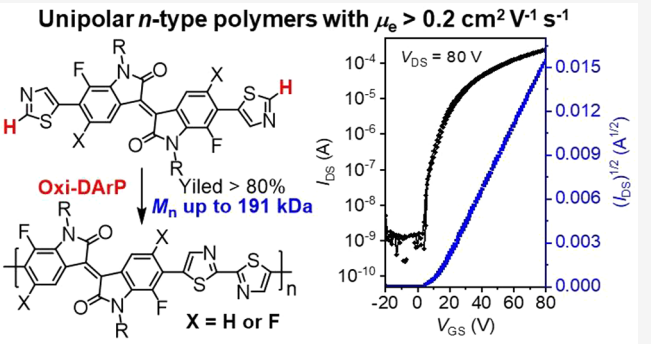

INTRODUCTION

Conjugated polymers (CPs) are an important embranchment of organic semiconductors. Taking advantage of the easily and finely adjustable chemical structures and thereby tunable properties, CPs can be endowed with a variety of characteristics to satisfy the demands of the wide applications in organic electronics, such as organic thin-film transistors (OTFTs), organic solar cells (OSCs), and organic electrochemical transistors (OECTs).[1−7]

The structurally diverse CPs are mostly constructed via polycondensation pathways based on transition-metal-catalyzed cross-coupling reactions.[8−12] In most cases, the reactions between organohalides (C−X) and organometallic reagents (C−M), e.g., Stille and Suzuki couplings, are adopted to synthesize the target CPs. Stille coupling as a typical method to form C−C bonds via the reactions between C−X substrates and organostannanes (C−SnR_3) can tolerate various functional groups and proceed efficiently in mild reaction conditions.[8] These features make Stille polycondensation a promising protocol for the synthesis of CPs with different functionality, except for the drawbacks of the tedious synthesis and purification procedure (less atom-economic) and highly toxic nature (environmentally unfriendly) of organostannanes.[10,13,14] Direct arylation polycondensation (DArP) of C−Br and C−H monomers is recently emerging as a new method for the synthesis of CPs.[13−20] Compared with traditional cross-coupling polycondensations of C−X and C−M monomers, DArP is more atom-economic and eco-friendly. With specially designed highly reactive C−H monomers, various high molecular weight CPs with superior electronic properties have been synthesized.[21−33]

C−H/C−H oxidative direct arylation polycondensation (Oxi-DArP) via the direct activation of C−H bonds in (hetero)arenes is the most straightforward and eco-friendly approach for the synthesis of CPs to date because no prefunctionalization or preactivation of monomers is necessary.[34−51] Some CPs have been successfully synthesized via Oxi-DArP. For instance, 2,2′-bithiazole-containing CPs have been synthesized by You and Kanbara via Pd- and Cu-catalyzed Oxi-DArP, respectively.[39,42] Nakamura et al.

Received: February 18, 2024
Revised: April 7, 2024
Accepted: April 11, 2024
Published: April 24, 2024

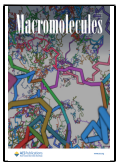

https://doi.org/10.1021/acs.macromol.4c00399
Macromolecules 2024, 57, 4158−4166

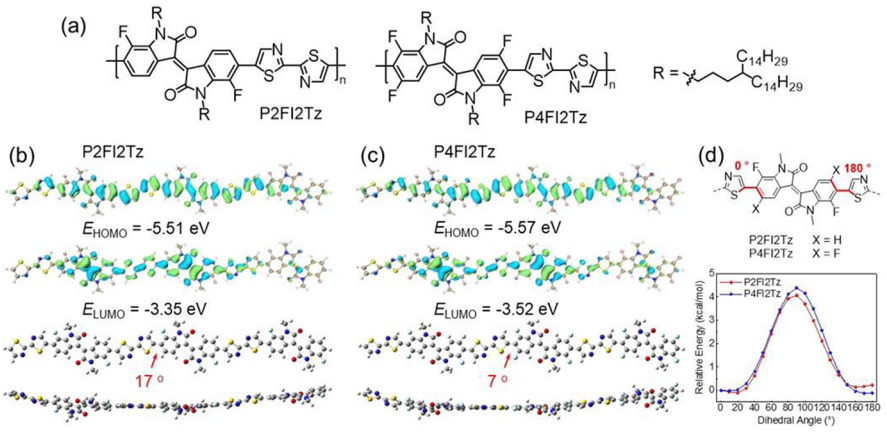

Figure 1. (a) Chemical structures of P2FI2Tz and P4FI2Tz. Optimized trimer structures along with calculated LUMO and HOMO energy levels and distribution of (b) P2FI2Tz and (c) P4FI2Tz and (d) dihedral torsion potentials of methyl-substituted repeating units. DFT calculations were carried out at the B3LYP-D3/6-31G(d,p) level.

synthesized triarylamine/bithiophene copolymers through Fe-catalyzed Oxi-DArP, which was used as hole transport materials for the fabrication of efficient perovskite solar cells.[47,48] Compared with C−Br/C−H DArP, Oxi-DArP is more straightforward since no prefunctionalized C−Br monomer is necessary.[50,51] However, the progress of Oxi-DArP has trailed much behind DArP because only a limited number of (hetero)arenes can undergo transition-metal-catalyzed oxidative C−H/C−H coupling efficiently to ensure the formation of high molecular weight products. There is also a lack of a design strategy to C−H monomers toward high-mobility CPs via Oxi-DArP. The C_2−H bond in thiazole is highly reactive in oxidative C−H/C−H coupling, allowing the synthesis of thiazole-containing CPs via Oxi-DArP.[39,42] More recently, we found that thiazol-5-yl-flanked aryls could undergo Oxi-DArP efficiently in toluene and chlorobenzene, which are good solvents of most polymer semiconductors.[49] A diketopyrrolopyrrole-based n-type CP with number-average molecular weight (M_n) above 20 kDa was successfully synthesized.

The development of n-type CPs lags much behind that of p-type counterparts. Isoindigo (IID), characterized by a planar and electron-deficient nature, is widely used in the construction of high-mobility CPs nowadays.[52−56] Its electron deficiency can be further strengthened via introducing fluoride (F) substituents or replacing phenyl moieties with pyridine rings, leading to the building blocks of n-type CPs.[22,29,57−60] Thiazole is also an electron-deficient heteroarene that has been frequently used in the synthesis of n-type CPs.[25,49,61−64] Moreover, its five-membered ring structure comprising an imine nitrogen atom brings a small steric hindrance, thus endowing resultant CPs with moderate to good planarity.[49,61−63] Combining the above features of IID derivatives and thiazole and the high oxidative C−H/C−H coupling reactivity of the C_2−H bond in thiazole as aforementioned, we synthesized two n-type CPs comprising alternatively arranged IID and bithiazole units, namely, P2FI2Tz and P4FI2Tz, via Oxi-DArP in the current paper. P2FI2Tz was also synthesized via DArP and Stille polycondensation for comparison. These two polymers are characterized by deep frontier molecular orbital (FMO) levels, allowing the fabrication of unipolar n-type OTFTs with electron mobility (μ_e) up to 0.28 $cm^2 V^{-1} s^{-1}$. Oxi-DArP is more efficient than the other two approaches, and P2FI2Tz with an M_n above 40 kDa could be obtained in just 9 h, significantly shorter than 24 h with DArP and Stille polycondensation. The Oxi-DArP-made polymer also delivered slightly better semiconducting properties. This finding paves a way to synthesize novel high-performance polymer semiconductors efficiently.

RESULTS AND DISCUSSION

Design of the Monomers and Polymers. The chemical structures of two target polymers based on IID and 2,2′-bithiazole, i.e., P2FI2Tz and P4FI2Tz, are displayed in Figure 1a. Two and four F atoms are installed in the IID unit for P2FI2Tz and P4FI2Tz, respectively. The introduction of F atoms in IID not only can lower both the lowest unoccupied molecular orbital (LUMO) and the highest occupied molecular orbital (HOMO) of the resulting polymers but also can improve the planarity of the conjugated backbones due to the presence of weak intramolecular interaction.[65,66] In fact, IID with two F atoms, namely, 2FIID, has been proved as a promising building block of n-type high-mobility CPs.[22,29,60] Although IID with four F atoms, namely, 4FIID, has not been reported yet, one can expect that CPs based on it have even lower HOMO and LUMO compared with 2FIID-based counterparts, which are preferred for the design of unipolar n-type CPs.

To corroborate our design concept, FMO energy levels, FMO distribution, and optimum geometries of the methyl-substituted trimers of the polymers were investigated by density functional theory (DFT) calculations (Figure 1b and c). The FMOs of both polymers are well delocalized. The calculated LUMO/HOMO energy levels (E_{LUMO}/E_{HOMO}) are −3.35/−5.51 eV and −3.52/−5.57 eV for P2FI2Tz and P4FI2Tz, respectively. Since there are two more F atoms in each repeating unit, P4FI2Tz shows lower FMO energy levels compared with P2FI2Tz. In the optimum geometries, a slight twist is found between IID and thiazole units, with torsion angles of 17° for P2FI2Tz and 7° for P4FI2Tz. Figure 1d shows the dihedral torsion potentials of the methyl-substituted repeating units. There exists a ca. 20° torsion in the two dominant conformations of P2FI2Tz, while the value for P4FI2Tz is between 0° and 10°. The discrepancy in energies of the two dominant conformations of P4FI2Tz is also smaller than that of P2FI2Tz. These results indicate that P4FI2Tz should be more inclined toward planar conformation. We attribute this phenomenon to the additional F atoms in

https://doi.org/10.1021/acs.macromol.4c00399
Macromolecules 2024, 57, 4158−4166

P4FI2Tz, which might generate a weak F···S intramolecular interaction to improve the planarity of the conjugated backbone.

Synthesis of the Monomers and Polymers. Scheme 1 depicts the synthetic routes to thiazol-5-yl-flanked IID derivatives 2FIID2Tz and 4FIID2Tz as C−H monomers and corresponding CPs P2FI2Tz and P4FI2Tz via Oxi-DArP. Pd-catalyzed C−Br/C−H direct arylation coupling of 6,6′-dibromo-7,7′-difluoroisoindigo (2FIID, **1**) and 2-(triisopropylsilyl)thiazole (**2**) followed by removing triisopropylsilyl (TIPS) protecting groups with CF_3COOH afforded 2FIID2Tz in a two-step yield of 88%. The monomer 4FIID2Tz was unable to be prepared following the same procedure because we failed to synthesize 6,6′-dibromo-5,5′,7,7′-tetrafluoroisoindigo (4FIID) from the dimerization of 6-bromo-5,7-difluoroisatin (**3**) in the presence of hexaethylphosphorous triamide ($P(NEt_2)_3$), an efficient route for the synthesis of various IID derivatives.[67] The reductive dimerization of **3** only yielded a mixture of unknown products that were hard to purify and identify.

Scheme 1. Synthetic Routes to Thiazole-Flanked IID Monomers and IID-Based Polymers[a]

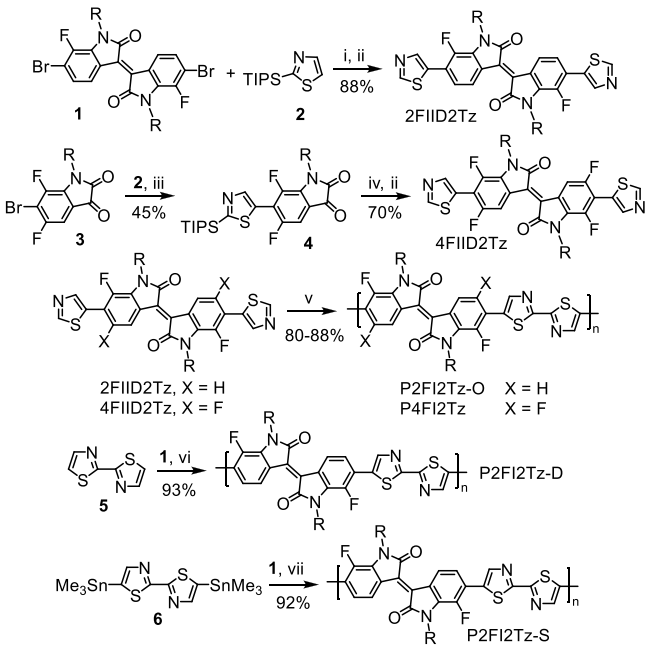

[a]Reagents and conditions: (i) Pd_2dba_3, P(*o*-MeOPh)$_3$, Cs_2CO_3, PivOH, toluene, 100 °C; (ii) CF_3COOH, $CHCl_3$, 45 °C; (iii) Pd_2dba_3, P(*o*-MeOPh)$_3$, K_2CO_3, PivOH, toluene, 100 °C; (iv) $P(NEt_2)_3$, CH_2Cl_2, −60 °C; (v) $PdCl_2$, CuCl, $Cu(OAc)_2$, chlorobenzene, 120 °C; (vi) Herrmann's cat., P(*o*-MeOPh)$_3$, Cs_2CO_3, PivOH, toluene, 120 °C; (vii) Pd_2dba_3, P(*o*-MePh)$_3$, toluene, 120 °C. TIPS: triisopropylsilyl. R: 4-tetradecyloctadecyl.

According to the mechanism of isatin dimerization to the IID structure proposed in the literature,[67] $P(NEt_2)_3$ functions as a nucleophilic reagent in the reaction (Figure S1a). Brinck et al. proposed a parameter named local electron attachment energy (E_{LEAE}) to evaluate the nucleophilic-attacking site in a compound.[68] The site with the most negative E_{LEAE} should be easily attacked by a nucleophilic reagent. As revealed by the calculated E_{LEAE} values of different sites in isatin derivatives MS1−MS3 (Figures S1b and S1c), the introduction of halogen atoms in the phenyl ring leads to a significant reduction of E_{LEAE} at the 6-position of the isatin skeleton. The E_{LEAE} at the 6-position of isatin **3**, which has three halogen substituents in the phenyl ring, is as low as −79.5 kcal mol^{-1}, very close to the value at the desired carbonyl site (−85.4 kcal mol^{-1}). Then we speculate that the phenyl ring in **3** is also susceptible to the nucleophilic attack in the dimerization of **3**, leading to a mixture of unknown products.

From the calculation, we also realized that replacing Br in **3** with 2-triisopropylsilylthiazole could solve the problem. As shown in Figure S1c, the E_{LEAE} at the 6-position of isatin in 5,7-difluoro-6-(2-(triisopropylsilyl)thiazol-5-yl)isatin (**4**) is −24.5 kcal mol^{-1}, much higher than the value (−78.2 kcal mol^{-1}) at the 3-position (carbonyl site). Along this line, compound **4** was first synthesized via C−Br/C−H direct arylation coupling in a moderate yield of 45%. Subsequent dimerization and deprotection successfully afforded the monomer 4FIID2Tz in a yield of 70%.

The Oxi-DArP of 2FIID2Tz and 4FIID2Tz was conducted in chlorobenzene with $PdCl_2$/CuCl/$Cu(OAc)_2$ as catalytic system.[49] Given that IID-based CPs often exhibit strong aggregation in solution, a relatively low monomer concentration of 0.02 mol L^{-1} was adopted in order to obtain high molecular weight products. First, the Oxi-DArP of 2FIID2Tz was conducted in different polycondensation times. The polymers with M_ns of 47, 59, and 191 kDa (named P2FI2Tz-O1, P2FI2Tz-O2, and P2FI2Tz-O3), respectively, were obtained in 9, 12, and 16 h (Table 1). Further enhancing the molecular weight of the polymer by extending polymerization time is difficult due to the decreased solubility along

Table 1. Polycondensation Results and Photophysical and Electrochemical Properties of the Resulting Polymers

					λ_{max} (nm)				
polymer	method[a]	*t* (h)	yield (%)[b]	M_n (kDa)/$Đ$[c]	solution	film	E_g (eV)	E_{LUMO} (eV)[d]	E_{HOMO} (eV)[d]
P2FI2Tz-O1	Oxi-DArP	9	82	47/2.0	662	671	1.69	−3.69	−6.01
P2FI2Tz-O2	Oxi-DArP	12	87	59/2.4	662	671	1.70	−3.68	−6.03
P2FI2Tz-O3	Oxi-DArP	16	88	191/3.2	660	664	1.70	−3.68	−6.05
P2FI2Tz-D	DArP	24	93	45/1.7	662	669	1.70	−3.70	−6.02
P2FI2Tz-S	Stille	24	92	47/2.0	662	670	1.69	−3.68	−6.04
P4FI2Tz	Oxi-DArP	18	80	87/1.8	634	673	1.65	−3.82	−6.24

[a]The monomer concentration is 0.02 mol L^{-1} for all polymerizations. [b]Yields after Soxhlet extraction. [c]Number-average molecular weight (M_n) and polydispersity index ($Đ$) measured by high-temperature (150 °C) gel permeation chromatography (GPC) with 1,2,4-trichlorobenzene as eluent and polystyrene as standard. [d]E_{LUMO} and E_{HOMO} were calculated according to $E_{LUMO} = -(4.40 + E_{re})$ eV and $E_{HOMO} = -(4.40 + E_{ox})$ eV, in which E_{re} and E_{ox} represent reduction and oxidation onset potentials of the polymers versus SCE, respectively. Oxi-DArP: oxidative direct arylation polycondensation. DArP: direct arylation polycondensation. Stille: Stille polycondensation.

https://doi.org/10.1021/acs.macromol.4c00399
Macromolecules 2024, 57, 4158−4166

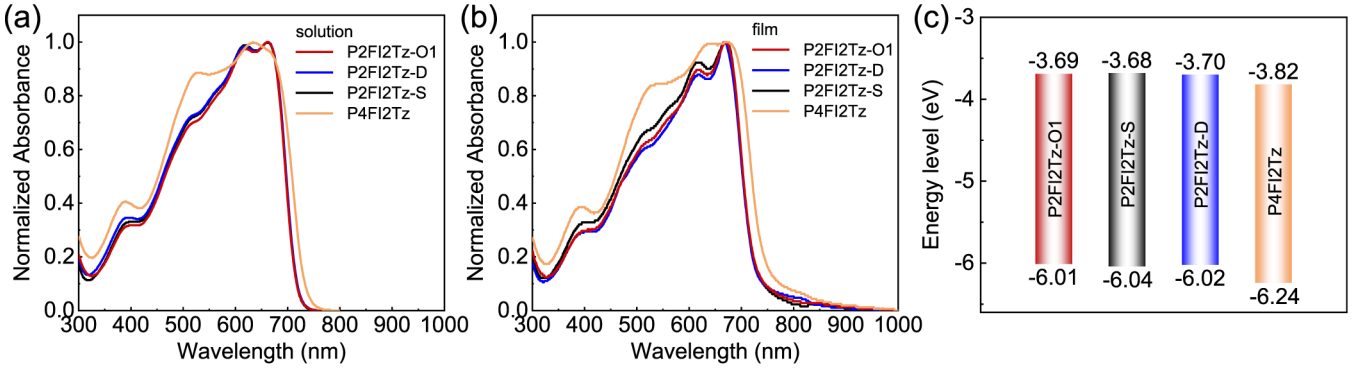

Figure 2. (a) Solution and (b) film UV−vis−NIR absorption spectra and (c) FMO energy levels diagram of the polymers. Solution absorption spectra were measured in chlorobenzene with a repeating unit concentration of 10^{-5} mol L^{-1}; films were prepared by spin-casting chlorobenzene solutions on quartz substrates.

with an enhancement of molecular weight, and the reaction system reached complete gelation in 16 h. Under the same Oxi-DArP condition, P4FI2Tz with an M_n of 87 kDa could be acquired in 18 h. These results demonstrate the great efficiency of Oxi-DArP in the synthesis of high molecular weight IID-based CPs. Note that P4FI2Tz is difficult to synthesize via other protocols such as DArP and Stille polycondensation, owing to the difficult synthesis of 4FIID C−Br monomers.

C−H bonds at the 5,5′-positions of 2,2′-bithiazole exhibit moderate direct arylation reactivity, and 5,5′-bis-(trimethylstannyl)-2,2′-bithiazole is accessible.[60,64] Then, for comparison, P2FI2Tz was also synthesized via DArP and Stille polycondensation as shown in Scheme 1. The resultant polymers are denoted as P2FI2Tz-D and P2FI2Tz-S, respectively. For fair comparison, the same monomer concentration (0.02 mol L^{-1}) was adopted. For both DArP and Stille polycondensation, a longer polymerization time was required to obtain high molecular weight products, while compared to Oxi-DArP, P2FI2Tz samples with M_ns below 40 kDa were obtained for both Stille polycondensation and DArP in 9 h (Table S1). By extending the polymerization time to 24 h, P2FI2Tz-D and P2FI2Tz-S with M_ns of 45 and 47 kDa, respectively, comparable to that of P2FI2Tz-O1, were obtained (Table 1). This polymerization time is much longer than 9 h used in Oxi-DArP to attain P2FI2Tz with comparable molecular weight. The above results further demonstrate the advantages of Oxi-DArP among different protocols in synthesizing CPs with the same repeating unit in terms of efficiency.

Other than chemical structures, the properties of CPs also correlate with their molecular weights. The successful synthesis of the same polymer with comparable molecular weight via three different methods allows for a fair comparison of the properties of the CPs from Oxi-DArP, DArP, and Stille polycondensation for the first time. Thus, following properties investigation will mainly focus on four CPs, i.e., P2FI2Tz-O1, P2FI2Tz-D, P2FI2Tz-S, and P4FI2Tz.

Thermal, Photophysical, and Electrochemical Properties of the Polymers. Thermal properties of the polymers were studied by thermogravimetric analysis (TGA) and differential scanning calorimetry (DSC). All four polymers P2FI2Tz-O1, P2FI2Tz-D, P2FI2Tz-S, and P4FI2Tz are thermally stable with 5 wt % decomposition temperatures (T_d) above 390 °C, as shown in Figure S2a. Only one thermal transition around 0 °C attributed to alkyl melting can be observed in DSC curves of the four polymers (Figure S2b), like previously reported IID-based CPs with the same alkyl side chains.[22,32]

Solution and film UV−vis−NIR absorption spectra are presented in Figure 2a and b, respectively, and the corresponding data are summarized in Table 1. As shown in Figure 2a, P2FI2Tz-O1, P2FI2Tz-D, and P2FI2Tz-S share overlapped solution absorption spectra, with an absorption maximum (λ_{max}) at 662 nm. Their film absorption spectra are also identical with the slightly red-shifted λ_{max}s of ∼670 nm and optical bandgaps (E_gs) of ∼1.70 eV. These indicate that the polymers synthesized via three methods (i.e., Oxi-DArP, DArP, and Stille polycondensation) exhibit similar photophysical properties. P2FI2Tz-O1, P2FI2Tz-O2, and P2FI2Tz-O3, which have different molecular weights, also show similar absorption spectra (Figure S3), indicating that the effective conjugated length is already reached at the M_n of ca. 47 kDa for P2FI2Tz. P4FI2Tz shows broad and featureless absorption spectra in both the solution and film state with a film E_g of 1.65 eV. Like other IID-based CPs reported in the literature,[22,29,32] there exists preaggregation in solution, which is supported by the temperature-dependent absorption spectra (Figure S4).

The E_{LUMO}s and E_{HOMO}s of the polymers were estimated from the redox onset potentials in cyclic voltammograms (CV, Figure S5). As shown in Figure 2c and Table 1, the E_{LUMO}/E_{HOMO} values are −3.69/−6.01 eV for P2FI2Tz-O1, −3.68/−6.03 eV for P2FI2Tz-O2, −3.68/−6.05 eV for P2FI2Tz-O3, −3.70/−6.02 eV for P2FI2Tz-D, and −3.68/−6.04 eV for P2FI2Tz-S. The FMO energy levels of P2FI2Tz samples obtained from three polycondensation methods are almost identical, and no obvious variation was observed for Oxi-DArP-made P2FI2Tz with different M_n. As expected, both the E_{LUMO} and E_{HOMO} of P4FI2Tz (−3.82/−6.24 eV) are obviously lower than those of P2FI2Tz due to more electron-withdrawing F atoms in the backbone of P4FI2Tz. The decrease trend of the HOMO/LUMO with the introduction of more F atoms in the conjugated backbone is in accordance with DFT calculations (Figure 1). It is worth noting that both P2FI2Tz and P4FI2Tz exhibit E_{HOMO} values < −6.0 eV, which is beneficial for suppressing the hole injection, thus enabling unipolar n-type transport in OTFTs.[69]

Semiconducting Properties of the Polymers. Top-gate and bottom-contact (TGBC) OTFTs were fabricated to evaluate the charge transport properties of the polymers. The precleaned highly n-doped Si/SiO_2 wafer was used as the substrate, and Au was used as the source and drain electrodes. No substrate or electrode modification was adopted. The

https://doi.org/10.1021/acs.macromol.4c00399
Macromolecules 2024, 57, 4158−4166

semiconductor layer was deposited using spin coating followed by thermal annealing at 150 °C for 10 min. The measurements of the electrical characteristics of the devices were conducted in ambient conditions, and the related data are summarized in Table 2. The μ_e values were extracted from the saturation regime. All polymers exhibited unipolar n-type transport properties. Figure 3 shows the typical transfer and output characteristics of OTFTs based on P2FI2Tz-O1, P2FI2Tz-D, P2FI2Tz-S, and P4FI2Tz. Obvious linear and saturation regimes can be observed in output curves, and $(I_{DS})^{1/2}$ linearly correlates with gate voltage (V_{GS}), as shown in transfer curves. The OTFTs based on P2FI2Tz-O1, P2FI2Tz-D, and P2FI2Tz-S showed a maximum μ_e ($\mu_{e,max}$) of 0.27, 0.23, and 0.24 cm^2 V^{-1} s^{-1}, respectively, with an on/off current ratio (I_{on}/I_{off}) of 10^4–10^5. The OTFT performance of P2FI2Tz-O2 was similar to that of P2FI2Tz-O1, showing a $\mu_{e,max}$ of 0.28 cm^2 V^{-1} s^{-1}. However, the $\mu_{e,max}$ of P2FI2Tz-O3 dropped drastically to 0.09 cm^2 V^{-1} s^{-1} (Figure S6 and Table S2). We ascribe the remarkably lower μ_e of P2FI2Tz-O3 to its very high molecular weight (M_n: 191 kDa), which might cause a disordered molecular packing in the film state.[70−72] The obvious reduction of charge transport properties as molecular weight increases was also observed before for other high-mobility CPs.[70,71] OTFTs based on P4FI2Tz demonstrated virtually ideal transfer and output characteristics with no obvious hysteresis, showing a slightly lower $\mu_{e,max}$ of 0.22 cm^2 V^{-1} s^{-1}. Noteworthily, the devices showed a much lower threshold voltage (V_{th}) of 10 to 12 V and higher I_{on}/I_{off} of 10^5–10^6, compared to the devices based on P2FI2Tz. These results are possibly attributed to the low enough E_{LUMO}/E_{HOMO} (−3.82/−6.24 eV) of P4FI2Tz, which can significantly suppress hole injection and encourage electron injection from the gold source to the semiconducting layer.

Table 2. OTFT Performances of P2FI2Tz and P4FI2Tz

polymer	$\mu_{e,max}$ ($\mu_{e,ave}$) (cm^{-2} V^{-1} s^{-1})[a]	V_{th} (V)	I_{on}/I_{off}
P2FI2Tz-O1	0.27 (0.24 ± 0.03)	20−25	10^4–10^5
P2FI2Tz-D	0.23 (0.22 ± 0.02)	30−34	10^4–10^5
P2FI2Tz-S	0.24 (0.22 ± 0.02)	34−35	10^4–10^5
P4FI2Tz	0.22 (0.19 ± 0.01)	10−12	10^5–10^6

[a]Maximum electron mobility extracted from the saturation regime with the average value from at least 6 devices given in parentheses.

Film Morphology and Microstructures. The film morphology and microstructures were characterized by tapping-mode atomic force microscopy (AFM) and grazing incidence X-ray diffraction (XRD). As shown in Figure 4a, the films of P2FI2Tz-O1, P2FI2Tz-D, P2FI2Tz-S, and P4FI2Tz, featuring similar granular morphology, were all continuous and uniform with the root-mean-square surface roughness (RMS) of 1.2−1.5 nm. Figure 4b displays film XRD profiles of P2FI2Tz-O1, P2FI2Tz-D, P2FI2Tz-S, and P4FI2Tz. All four polymers showed similar XRD patterns. Sharp (h00) diffraction peaks up to fourth order along with a broad (010) diffraction peak were observed in the out-of-plane pattern, while only a weak (100) peak was visible in the in-plane direction. This means that the conjugated backbones of the four CPs adopted an edge-on/face-on bimodal packing. The lamellar d-spacings and π−π stacking distances derived from (100) and (010) peaks (~29 Å and 3.46−3.48 Å, respectively) and corresponding lamellar stacking coherence lengths (Table S3) were also similar. All these results are consistent with the close OTFT performance of the four polymers.

Film AFM images and XRD profiles of P2FI2Tz-O2 and P2FI2Tz-O3 were also recorded. As shown in Figure S7, the film AFM images and XRD profiles of P2FI2Tz-O2 were identical to those of P2FI2Tz-O1, consistent with their similar OTFT performance. In contrast, the P2FI2Tz-O3 film

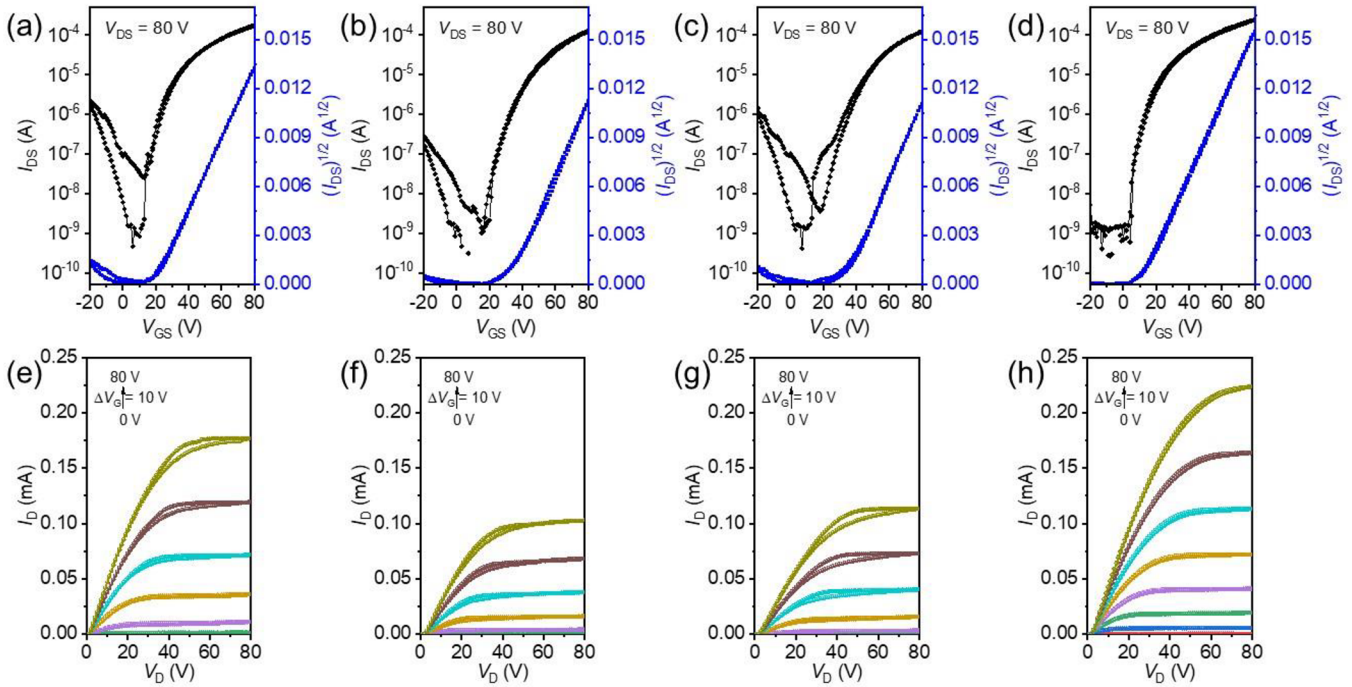

Figure 3. Typical (a−d) transfer and (e−h) output characteristics of TGBC OTFTs based on (a, e) P2FI2Tz-O1, (b, f) P2FI2Tz-D, (c, g) P2FI2Tz-S, and (d, h) P4FI2Tz.

https://doi.org/10.1021/acs.macromol.4c00399
Macromolecules 2024, 57, 4158−4166

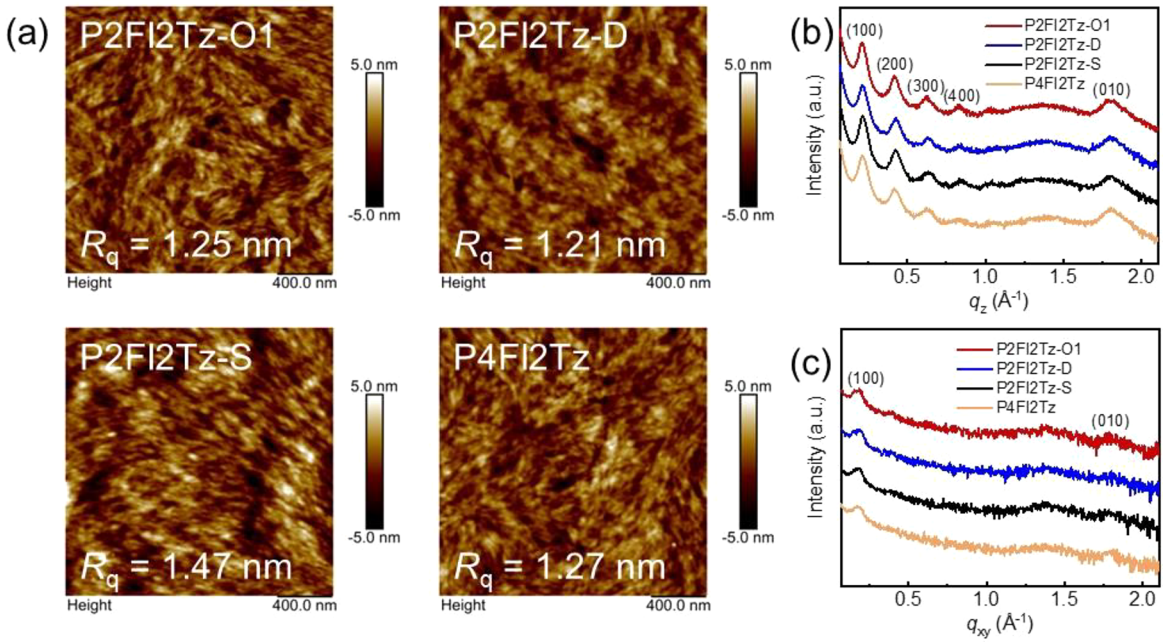

Figure 4. AFM height images (a, 2 μm × 2 μm) and out-of-plane (b) and in-plane (c) XRD profiles of the spin-cast polymer films. All films were prepared in the same way as those for the fabrication of OTFT devices.

exhibited much weaker diffraction peaks in XRD patterns along with smaller domain sizes in AFM images. These features are inferior to charge transport and match well with the remarkably lower mobility of P2FI2Tz-O3. Low packing order of P2FI2Tz-O3 can be ascribed to the poor self-assembly originated from its very high molecular weight.[70−72]

CONCLUSIONS

In summary, we designed and synthesized two thiazole-flanked multifluorinated IID derivatives, 2FIID2Tz and 4FIID2Tz, and their corresponding CPs, P2FI2Tz and P4FI2Tz, were synthesized via Oxi-DArP. Both polymers are unipolar n-type CPs with μ_e above 0.2 cm^2 V^{-1} s^{-1}, attributed to their low HOMO and LUMO levels. Compared with P2FI2Tz, P4FI2Tz has decreased HOMO/LUMO levels due to more electron-withdrawing F atoms in its backbone. Thereby, the devices based on P4FI2Tz exhibited much lower V_{th} and higher I_{on}/I_{off}. Compared with DArP and Stille polycondensation, which were also used for the synthesis of P2FI2Tz, Oxi-DArP is more efficient, and the polymer with M_n above 40 kDa could be synthesized with a polymerization time as short as 9 h. In addition, Oxi-DArP-made P2FI2Tz showed slightly better OTFT performance, and P4FI2Tz could only be made via Oxi-DArP, not through the other two protocols. This study provides a design strategy of C−H monomers to make high-mobility n-type CPs via Oxi-DArP and demonstrates that Oxi-DArP is a concise and effective pathway to CPs for electronic applications.

ASSOCIATED CONTENT

Supporting Information

The Supporting Information is available free of charge at https://pubs.acs.org/doi/10.1021/acs.macromol.4c00399.

General methods, synthetic procedures, NMR spectra, GPC curves, and other supplementary data (PDF)

AUTHOR INFORMATION

Corresponding Authors

Yunfeng Deng − *School of Materials Science and Engineering and Tianjin Key Laboratory of Molecular Optoelectronic Science, Tianjin University, Key Laboratory of Organic Integrated Circuits, Ministry of Education, and Collaborative Innovation Center of Chemical Science and Engineering (Tianjin), Tianjin 300072, People's Republic of China;* orcid.org/0000-0003-0479-2976; Email: yunfeng.deng@tju.edu.cn

Yanhou Geng − *School of Materials Science and Engineering and Tianjin Key Laboratory of Molecular Optoelectronic Science, Tianjin University, Key Laboratory of Organic Integrated Circuits, Ministry of Education, and Collaborative Innovation Center of Chemical Science and Engineering (Tianjin), Tianjin 300072, People's Republic of China; Joint School of National University of Singapore and Tianjin University, International Campus of Tianjin University, Binhai New City, Fuzhou 350207, People's Republic of China;* orcid.org/0000-0002-4997-3925; Email: yanhou.geng@tju.edu.cn

Authors

Yibo Shi − *School of Materials Science and Engineering and Tianjin Key Laboratory of Molecular Optoelectronic Science, Tianjin University, Key Laboratory of Organic Integrated Circuits, Ministry of Education, and Collaborative Innovation Center of Chemical Science and Engineering (Tianjin), Tianjin 300072, People's Republic of China*

Xuwen Zhang − *School of Materials Science and Engineering and Tianjin Key Laboratory of Molecular Optoelectronic Science, Tianjin University, Key Laboratory of Organic Integrated Circuits, Ministry of Education, and Collaborative Innovation Center of Chemical Science and Engineering (Tianjin), Tianjin 300072, People's Republic of China*

Tianzuo Wang − *School of Materials Science and Engineering and Tianjin Key Laboratory of Molecular Optoelectronic*

https://doi.org/10.1021/acs.macromol.4c00399
Macromolecules 2024, 57, 4158−4166

Science, Tianjin University, Key Laboratory of Organic Integrated Circuits, Ministry of Education, and Collaborative Innovation Center of Chemical Science and Engineering (Tianjin), Tianjin 300072, People's Republic of China

Mei Rao − *School of Materials Science and Engineering and Tianjin Key Laboratory of Molecular Optoelectronic Science, Tianjin University, Key Laboratory of Organic Integrated Circuits, Ministry of Education, and Collaborative Innovation Center of Chemical Science and Engineering (Tianjin), Tianjin 300072, People's Republic of China*

Yang Han − *School of Materials Science and Engineering and Tianjin Key Laboratory of Molecular Optoelectronic Science, Tianjin University, Key Laboratory of Organic Integrated Circuits, Ministry of Education, and Collaborative Innovation Center of Chemical Science and Engineering (Tianjin), Tianjin 300072, People's Republic of China;* orcid.org/0000-0003-4248-6072

Complete contact information is available at: https://pubs.acs.org/10.1021/acs.macromol.4c00399

Author Contributions

Y.S., Y.D., and Y.G. conceived the project and designed the experiments. Y.S. mainly carried out the synthesis, characterization, and other experiments in this work. X.Z., T.W., and M.R. helped with the synthesis and characterization of the monomers and polymers. Y.H. helped with the organization of the manuscript. Y.S., Y.D. and Y.G. cowrote the paper, and all authors listed reviewed and commented on the manuscript.

Notes

The authors declare no competing financial interest.

■ ACKNOWLEDGMENTS

This work is supported by the National Key R&D Program (No. 2022YFB3603800) of the Chinese Ministry of Science and Technology, National Natural Science Foundation of China (Nos. 51933008 and 52121002), and the Fundamental Research Funds for the Central Universities.

■ REFERENCES

(1) Yang, J.; Zhao, Z.; Wang, S.; Guo, Y.; Liu, Y. Insight into High-Performance Conjugated Polymers for Organic Field-Effect Transistors. *Chem.* **2018**, *4*, 2748−2785.

(2) Rivnay, J.; Inal, S.; Salleo, A.; Owens, R. M.; Berggren, M.; Malliaras, G. G. Organic Electrochemical Transistors. *Nat. Rev. Mater.* **2018**, *3*, 17086.

(3) Bronstein, H.; Nielsen, C. B.; Schroeder, B. C.; McCulloch, I. The Role of Chemical Design in the Performance of Organic Semiconductors. *Nat. Rev. Chem.* **2020**, *4*, 66−77.

(4) Li, Y.-F.; Guo, Y.-L.; Liu, Y.-Q. Recent Progress in Donor-Acceptor Type Conjugated Polymers for Organic Field-effect Transistors. *Chin. J. Polym. Sci.* **2023**, *41*, 652−670.

(5) Kim, M.; Ryu, S. U.; Park, S. A.; Choi, K.; Kim, T.; Chung, D.; Park, T. Donor−Acceptor-Conjugated Polymer for High-Performance Organic Field-Effect Transistors: A Progress Report. *Adv. Funct. Mater.* **2020**, *30*, No. 1904545.

(6) Fu, H.; Wang, Z.; Sun, Y. Polymer Donors for High-Performance Non-Fullerene Organic Solar Cells. *Angew. Chem., Int. Ed.* **2019**, *58*, 4442−4453.

(7) Wang, G.; Melkonyan, F. S.; Facchetti, A.; Marks, T. J. All-Polymer Solar Cells: Recent Progress, Challenges, and Prospects. *Angew. Chem., Int. Ed.* **2019**, *58*, 4129−4142.

(8) Carsten, B.; He, F.; Son, H. J.; Xu, T.; Yu, L. Stille Polycondensation for Synthesis of Functional Materials. *Chem. Rev.* **2011**, *111*, 1493−1528.

(9) Sakamoto, J.; Rehahn, M.; Wegner, G.; Schluter, A. D. Suzuki Polycondensation: Polyarylenes a la Carte. *Macromol. Rapid Commun.* **2009**, *30*, 653−687.

(10) Ran, Y.; Guo, Y.; Liu, Y. Organostannane-Free Polycondensation and Eco-Friendly Processing Strategy for the Design of Semiconducting Polymers in Transistors. *Mater. Horiz.* **2020**, *7*, 1955−1970.

(11) Ding, L.; Yu, Z. D.; Wang, X. Y.; Yao, Z. F.; Lu, Y.; Yang, C. Y.; Wang, J. Y.; Pei, J. Polymer Semiconductors: Synthesis, Processing, and Applications. *Chem. Rev.* **2023**, *123*, 7421−7497.

(12) Xu, C.; Dong, J.; He, C.; Yun, J.; Pan, X. Precise Control of Conjugated Polymer Synthesis from Step-Growth Polymerization to Iterative Synthesis. *Giant* **2023**, *14*, No. 100154.

(13) Bura, T.; Blaskovits, J. T.; Leclerc, M. Direct (Hetero)arylation Polymerization: Trends and Perspectives. *J. Am. Chem. Soc.* **2016**, *138*, 10056−10071.

(14) Pouliot, J. R.; Grenier, F.; Blaskovits, J. T.; Beaupre, S.; Leclerc, M. Direct (Hetero)arylation Polymerization: Simplicity for Conjugated Polymer Synthesis. *Chem. Rev.* **2016**, *116*, 14225−14274.

(15) Mercier, L. G.; Leclerc, M. Direct (Hetero)arylation: A New Tool for Polymer Chemists. *Acc. Chem. Res.* **2013**, *46*, 1597−1605.

(16) Okamoto, K.; Zhang, J.; Housekeeper, J. B.; Marder, S. R.; Luscombe, C. K. C−H Arylation Reaction: Atom Efficient and Greener Syntheses of π-Conjugated Small Molecules and Macromolecules for Organic Electronic Materials. *Macromolecules* **2013**, *46*, 8059−8078.

(17) Mayhugh, A. L.; Yadav, P.; Luscombe, C. K. Circular Discovery in Small Molecule and Conjugated Polymer Synthetic Methodology. *J. Am. Chem. Soc.* **2022**, *144*, 6123−6135.

(18) Geng, Y. H.; Sui, Y. Direct Arylation Polycondensation Synthesis of High Mobility Conjugated Polymers. *Acta Polym. Sin.* **2019**, *50*, 109−117.

(19) Pankow, R. M.; Thompson, B. C. Approaches for Improving the Sustainability of Conjugated Polymer Synthesis Using Direct Arylation Polymerization (DArP). *Polym. Chem.* **2020**, *11*, 630−640.

(20) Gobalasingham, N. S.; Thompson, B. C. Direct Arylation Polymerization: A Guide to Optimal Conditions for Effective Conjugated Polymers. *Prog. Polym. Sci.* **2018**, *83*, 135−201.

(21) Bura, T.; Beaupré, S.; Ibraikulov, O. A.; Légaré, M.-A.; Quinn, J.; Lévêque, P.; Heiser, T.; Li, Y.; Leclerc, N.; Leclerc, M. New Fluorinated Dithienyldiketopyrrolopyrrole Monomers and Polymers for Organic Electronics. *Macromolecules* **2017**, *50*, 7080−7090.

(22) Gao, Y.; Deng, Y.; Tian, H.; Zhang, J.; Yan, D.; Geng, Y.; Wang, F. Multifluorination toward High-Mobility Ambipolar and Unipolar n-Type Donor-Acceptor Conjugated Polymers Based on Isoindigo. *Adv. Mater.* **2017**, *29*, No. 1606217.

(23) Gao, Y.; Bai, J.; Sui, Y.; Han, Y.; Deng, Y.; Tian, H.; Geng, Y.; Wang, F. High Mobility Ambipolar Diketopyrrolopyrrole-Based Conjugated Polymers Synthesized via Direct Arylation Polycondensation: Influence of Thiophene Moieties and Side Chains. *Macromolecules* **2018**, *51*, 8752−8760.

(24) Guo, K.; Bai, J.; Jiang, Y.; Wang, Z.; Sui, Y.; Deng, Y.; Han, Y.; Tian, H.; Geng, Y. Diketopyrrolopyrrole-Based Conjugated Polymers Synthesized via Direct Arylation Polycondensation for High Mobility Pure n-Channel Organic Field-Effect Transistors. *Adv. Funct. Mater.* **2018**, *28*, No. 1801097.

(25) Wang, Y.; Hasegawa, T.; Matsumoto, H.; Michinobu, T. Significant Difference in Semiconducting Properties of Isomeric All-Acceptor Polymers Synthesized via Direct Arylation Polycondensation. *Angew. Chem., Int. Ed.* **2019**, *58*, 11893−11902.

(26) Sui, Y.; Shi, Y.; Deng, Y.; Li, R.; Bai, J.; Wang, Z.; Dang, Y.; Han, Y.; Kirby, N.; Ye, L.; Geng, Y. Direct Arylation Polycondensation of Chlorinated Thiophene Derivatives to High-Mobility Conjugated Polymers. *Macromolecules* **2020**, *53*, 10147−10154.

(27) Shen, T.; Li, W.; Zhao, Y.; Liu, Y.; Wang, Y. An All-C−H-Activation Strategy to Rapidly Synthesize High-Mobility Well-Balanced Ambipolar Semiconducting Polymers. *Matter* **2022**, *5*, 1953−1968.

(28) Sui, Y.; Wang, Z.; Bai, J.; Shi, Y.; Zhang, X.; Deng, Y.; Han, Y.; Geng, Y. Diketopyrrolopyrrole-Based Conjugated Polymers Synthesized by Direct Arylation Polycondensation for Anisole-Processed High Mobility Organic Thin-Film Transistors. *J. Mater. Chem. C* **2022**, *10*, 2616−2622.
(29) Xu, C.; Wang, Z.; Dong, W.; He, C.; Shi, Y.; Bai, J.; Zhang, C.; Gao, M.; Jiang, H.; Deng, Y.; Ye, L.; Han, Y.; Geng, Y. Aggregation Behavior and Electrical Performance Control of Isoindigo-Based Conjugated Polymers via Carbosilane Side Chain Engineering. *Macromolecules* **2022**, *55*, 10385−10394.
(30) Zhang, X.; Shi, Y.; Dang, Y.; Liang, Z.; Wang, Z.; Deng, Y.; Han, Y.; Hu, W.; Geng, Y. Direct Arylation Polycondensation of β-Fluorinated Bithiophenes to Polythiophenes: Effect of Side Chains in C−Br Monomers. *Macromolecules* **2022**, *55*, 8095−8105.
(31) Zhang, X.; Shi, Y.; Deng, Y.; Geng, Y. Direct Arylation Polycondensation of Thiophene-Based C−H Monomers. *Chin. J. Chem.* **2023**, *41*, 2908−2924.
(32) Wang, P.; Xu, C.; Zhang, X.; Shi, Y.; Wang, C.; Han, Y.; Deng, Y.; Geng, Y. Thienoisoindigo-Based Conjugated Polymers Synthesized by Direct Arylation Polycondensation. *Macromol. Rapid Commun.* **2024**, *45*, No. 2300245.
(33) Zhang, C.; Tan, W. L.; Liu, Z.; He, Q.; Li, Y.; Ma, J.; Chesman, A. S. R.; Han, Y.; McNeill, C. R.; Heeney, M.; Fei, Z. High-Performance Unipolar n-Type Conjugated Polymers Enabled by Highly Electron-Deficient Building Blocks Containing F and CN Groups. *Macromolecules* **2022**, *55*, 4429−4440.
(34) Huang, Q.; Qin, X.; Li, B.; Lan, J.; Guo, Q.; You, J. Cu-Catalysed Oxidative C-H/C-H Coupling Polymerisation of Benzodiimidazoles: An Efficient Approach to Regioregular Polybenzodiimidazoles for Blue-Emitting Materials. *Chem. Commun.* **2014**, *50*, 13739−13741.
(35) Zhang, Q.; Wan, X.; Lu, Y.; Li, Y.; Li, Y.; Li, C.; Wu, H.; Chen, Y. The Synthesis of 5-Alkyl[3,4-c]thienopyrrole-4,6-dione-Based Polymers Using A Pd-Catalyzed Oxidative C-H/C-H Homopolymerization Reaction. *Chem. Commun.* **2014**, *50*, 12497−12499.
(36) Tsuchiya, K.; Ogino, K. Catalytic Oxidative Polymerization of Thiophene Derivatives. *Polym. J.* **2013**, *45*, 281−286.
(37) Zhang, Q.; Li, Y.; Lu, Y.; Zhang, H.; Li, M.; Yang, Y.; Wang, J.; Chen, Y.; Li, C. Pd-Catalysed Oxidative C−H/C−H Coupling Polymerization for Polythiazole-Based Derivatives. *Polymer* **2015**, *68*, 227−233.
(38) Gobalasingham, N. S.; Noh, S.; Thompson, B. C. Palladium-Catalyzed Oxidative Direct Arylation Polymerization (Oxi-DArP) of An Ester-Functionalized Thiophene. *Polym. Chem.* **2016**, *7*, 1623−1631.
(39) Guo, Q.; Jiang, R.; Wu, D.; You, J. Rapid Access to 2,2′-Bithiazole-Based Copolymers via Sequential Palladium-Catalyzed C-H/C-X and C-H/C-H Coupling Reactions. *Macromol. Rapid Commun.* **2016**, *37*, 794−798.
(40) Guo, Q.; Wu, D.; You, J. Oxidative Direct Arylation Polymerization Using Oxygen as the Sole Oxidant: Facile, Green Access to Bithiazole-Based Polymers. *ChemSusChem* **2016**, *9*, 2765−2768.
(41) Aoki, H.; Saito, H.; Shimoyama, Y.; Kuwabara, J.; Yasuda, T.; Kanbara, T. Synthesis of Conjugated Polymers Containing Octafluorobiphenylene Unit via Pd-Catalyzed Cross-Dehydrogenative-Coupling Reaction. *ACS Macro Lett.* **2018**, *7*, 90−94.
(42) Faradhiyani, A.; Zhang, Q.; Maruyama, K.; Kuwabara, J.; Yasuda, T.; Kanbara, T. Synthesis of Bithiazole-Based Semiconducting Polymers via Cu-Catalysed Aerobic Oxidative Coupling. *Mater. Chem. Front.* **2018**, *2*, 1306−1309.
(43) Zhang, Q.; Chang, M.; Lu, Y.; Sun, Y.; Li, C.; Yang, X.; Zhang, M.; Chen, Y. A Direct C−H Coupling Method for Preparing π-Conjugated Functional Polymers with High Regioregularity. *Macromolecules* **2018**, *51*, 379−388.
(44) Adamczak, D.; Komber, H.; Illy, A.; Scaccabarozzi, A. D.; Caironi, M.; Sommer, M. Indacenodithiophene Homopolymers via Direct Arylation: Direct Polycondensation versus Polymer Analogous Reaction Pathways. *Macromolecules* **2019**, *52*, 7251−7259.
(45) Collier, G. S.; Reynolds, J. R. Exploring the Utility of Buchwald Ligands for C-H Oxidative Direct Arylation Polymerizations. *ACS Macro Lett.* **2019**, *8*, 931−936.
(46) Kang, L. J.; Xing, L.; Luscombe, C. K. Exploration and Development of Gold- and Silver-Catalyzed Cross Dehydrogenative Coupling toward Donor−Acceptor π-Conjugated Polymer Synthesis. *Polym. Chem.* **2019**, *10*, 486−493.
(47) Doba, T.; Ilies, L.; Sato, W.; Shang, R.; Nakamura, E. Iron-catalysed regioselective thienyl C−H/C−H coupling. *Nat. Catal.* **2021**, *4*, 631−638.
(48) Lin, H. S.; Doba, T.; Sato, W.; Matsuo, Y.; Shang, R.; Nakamura, E. Triarylamine/Bithiophene Copolymer with Enhanced Quinoidal Character as Hole-Transporting Material for Perovskite Solar Cells. *Angew. Chem., Int. Ed.* **2022**, *61*, No. e202203949.
(49) Shi, Y.; Zhang, X.; Du, T.; Han, Y.; Deng, Y.; Geng, Y. A High-Performance n-Type Thermoelectric Polymer from C-H/C-H Oxidative Direct Arylation Polycondensation. *Angew. Chem., Int. Ed.* **2023**, *62*, No. e202219262.
(50) Chakraborty, B.; Luscombe, C. K. Cross-Dehydrogenative Coupling Polymerization via C-H Activation for the Synthesis of Conjugated Polymers. *Angew. Chem., Int. Ed.* **2023**, *62*, No. e202301247.
(51) Yang, Y.; Wu, Y.; Bin, Z.; Zhang, C.; Tan, G.; You, J. Discovery of Organic Optoelectronic Materials Powered by Oxidative Ar-H/Ar-H Coupling. *J. Am. Chem. Soc.* **2024**, *146*, 1224−1243.
(52) Zhu, M.; Guo, Y.; Liu, Y. A Thriving Decade: Rational Design, Green Synthesis, and Cutting-Edge Applications of Isoindigo-Based Conjugated Polymers in Organic Field-Effect Transistors. *Sci. China Chem.* **2022**, *65*, 1225−1264.
(53) Wan, X.; Li, B.; Mu, Y.; Li, L.; Luo, L. Synthesis of Nitrogen-Containing Isoindigo Derivatives and Their Applications in Optoelectronic Materials. *Chin. J. Org. Chem.* **2022**, *42*, 1960−1973.
(54) Randell, N. M.; Kelly, T. L. Recent Advances in Isoindigo-Inspired Organic Semiconductors. *Chem. Rec.* **2019**, *19*, 973−988.
(55) Wei, X.; Zhang, W.; Yu, G. Semiconducting Polymers Based on Isoindigo and Its Derivatives: Synthetic Tactics, Structural Modifications, and Applications. *Adv. Funct. Mater.* **2021**, *31*, No. 2010979.
(56) Lei, T.; Wang, J. Y.; Pei, J. Design, Synthesis, and Structure-Property Relationships of Isoindigo-Based Conjugated Polymers. *Acc. Chem. Res.* **2014**, *47*, 1117−1126.
(57) Guo, K.; Jiang, Y.; Sui, Y.; Deng, Y.-F.; Geng, Y.-H. Dimethylacetamide-Promoted Direct Arylation Polycondensation of 6,6′-Dibromo-7,7′-diazaisoindigo and (E)-1,2-bis(3,4-difluorothien-2-yl)ethene toward High Molecular Weight n-Type Conjugated Polymers. *Chin. J. Polym. Sci.* **2019**, *37*, 1099−1104.
(58) Wei, C.; Tang, Z.; Zhang, W.; Huang, J.; Zhou, Y.; Wang, L.; Yu, G. Molecular Engineering of (E)-1,2-Bis(3-cyanothiophene-2-yl)ethene-Based Polymeric Semiconductors for Unipolar n-Channel Field-Effect Transistors. *Polym. Chem.* **2020**, *11*, 7340−7348.
(59) Zhang, W.; Shi, K.; Lai, J.; Zhou, Y.; Wei, X.; Che, Q.; Wei, J.; Wang, L.; Yu, G. Record-High Electron Mobility Exceeding 16 $cm^2 V^{-1} s^{-1}$ in Bisisoindigo-Based Polymer Semiconductor with a Fully Locked Conjugated Backbone. *Adv. Mater.* **2023**, *35*, No. 2300145.
(60) Ran, Y.; Li, Q.; Li, J.; Sun, Y.; Shi, W.; Guo, Y.; Liu, Y. Nonchlorinated Solubility Enhanced by Lipophilicity: An Effective Strategy for Environmentally Benign Processing of Rigidly Regular n-type Polymeric Semiconductors. *Adv. Electron. Mater.* **2021**, *7*, No. 2100526.
(61) Shi, Y.; Li, J.; Sun, H.; Li, Y.; Wang, Y.; Wu, Z.; Jeong, S. Y.; Woo, H. Y.; Fabiano, S.; Guo, X. Thiazole Imide-Based All-Acceptor Homopolymer with Branched Ethylene Glycol Side Chains for Organic Thermoelectrics. *Angew. Chem., Int. Ed.* **2022**, *61*, No. e202214192.
(62) Zhang, L.; Wang, Z.; Duan, C.; Wang, Z.; Deng, Y.; Xu, J.; Huang, F.; Cao, Y. Conjugated Polymers Based on Thiazole Flanked Naphthalene Diimide for Unipolar n-Type Organic Field-Effect Transistors. *Chem. Mater.* **2018**, *30*, 8343−8351.

https://doi.org/10.1021/acs.macromol.4c00399
Macromolecules 2024, 57, 4158−4166

(63) Shi, Y.; Guo, H.; Qin, M.; Zhao, J.; Wang, Y.; Wang, H.; Wang, Y.; Facchetti, A.; Lu, X.; Guo, X. Thiazole Imide-Based All-Acceptor Homopolymer: Achieving High-Performance Unipolar Electron Transport in Organic Thin-Film Transistors. *Adv. Mater.* **2018**, *30*, No. 1705745.
(64) Yuan, Z.; Fu, B.; Thomas, S.; Zhang, S.; DeLuca, G.; Chang, R.; Lopez, L.; Fares, C.; Zhang, G.; Bredas, J.-L.; Reichmanis, E. Unipolar Electron Transport Polymers: A Thiazole Based All-Electron Acceptor Approach. *Chem. Mater.* **2016**, *28*, 6045−6049.
(65) Jackson, N. E.; Savoie, B. M.; Kohlstedt, K. L.; Olvera de la Cruz, M.; Schatz, G. C.; Chen, L. X.; Ratner, M. A. Controlling Conformations of Conjugated Polymers and Small Molecules: the Role of Nonbonding Interactions. *J. Am. Chem. Soc.* **2013**, *135*, 10475−10483.
(66) Huang, H.; Yang, L.; Facchetti, A.; Marks, T. J. Organic and Polymeric Semiconductors Enhanced by Noncovalent Conformational Locks. *Chem. Rev.* **2017**, *117*, 10291−10318.
(67) Bogdanov, A.; Mironov, V.; Musin, L.; Musin, R. Facile Synthesis of 1,1′-Dialkylisoindigos through Deoxygenation Reaction of Isatins and Tris(diethylamino)phosphine. *Synthesis* **2010**, *2010*, 3268−3270.
(68) Brinck, T.; Carlqvist, P.; Stenlid, J. H. Local Electron Attachment Energy and Its Use for Predicting Nucleophilic Reactions and Halogen Bonding. *J. Phys. Chem. A* **2016**, *120*, 10023−10032.
(69) Chen, F.; Jiang, Y.; Sui, Y.; Zhang, J.; Tian, H.; Han, Y.; Deng, Y.; Hu, W.; Geng, Y. Donor−Acceptor Conjugated Polymers Based on Bisisoindigo: Energy Level Modulation toward Unipolar n-Type Semiconductors. *Macromolecules* **2018**, *51*, 8652−8661.
(70) Wang, Z.; Gao, M.; He, C.; Shi, W.; Deng, Y.; Han, Y.; Ye, L.; Geng, Y. Unraveling the Molar Mass Dependence of Shearing-Induced Aggregation Structure of a High-Mobility Polymer Semiconductor. *Adv. Mater.* **2022**, *34*, No. 2108255.
(71) Pei, D.; Wang, Z.; Peng, Z.; Zhang, J.; Deng, Y.; Han, Y.; Ye, L.; Geng, Y. Impact of Molecular Weight on the Mechanical and Electrical Properties of a High-Mobility Diketopyrrolopyrrole-Based Conjugated Polymer. *Macromolecules* **2020**, *53*, 4490−4500.
(72) Huang, G.; Wu, N.; Wang, X.; Zhang, G.; Qiu, L. Role of Molecular Weight in the Mechanical Properties and Charge Transport of Conjugated Polymers Containing Siloxane Side Chains. *Macromol. Rapid Commun.* **2022**, *43*, No. 2200149.

https://doi.org/10.1021/acs.macromol.4c00399
Macromolecules 2024, 57, 4158−4166